JACS
JOURNAL OF THE AMERICAN CHEMICAL SOCIETY

Communication

pubs.acs.org/JACS

Metal-to-Metal Electron Transfer in Co/Fe Prussian Blue Molecular Analogues: The Ultimate Miniaturization

Evangelia S. Koumousi,[†,‡,§,#] Ie-Rang Jeon,[†,‡,§,#] Qian Gao,[⊥] Pierre Dechambenoit,[†,‡] Daniel N. Woodruff,[†,‡] Pascal Merzeau,[†,‡] Lionel Buisson,[†,‡] Xiaolu Jia,[⊥] Dongfeng Li,*[,⊥] Florence Volatron,[∥] Corine Mathonière,*[,§,#] and Rodolphe Clérac*[,†,‡]

[†]CNRS, CRPP, UPR 8641, F-33600 Pessac, France

[‡]Univ. Bordeaux, CRPP, UPR 8641, F-33600 Pessac, France

[§]CNRS, ICMCB, UPR 9048, F-33600 Pessac, France

[#]Univ. Bordeaux, ICMCB, UPR 9048, F-33600 Pessac, France

[⊥]College of Chemistry, Key Laboratory of Pesticide and Chemical Biology of Ministry of Education, Central China Normal University (CCNU), 430079 Wuhan, P. R. China

[∥]Université Pierre et Marie Curie Paris 6, 75252 Paris cedex 5, France

Supporting Information

ABSTRACT: Co/Fe Prussian Blue analogues are known to display both thermally and light induced electron transfer attributed to the switching between diamagnetic $\{Fe^{II}_{LS}(\mu\text{-CN})Co^{III}_{LS}\}$ and paramagnetic $\{Fe^{III}_{LS}(\mu\text{-CN})Co^{II}_{HS}\}$ pairs (LS = low spin; HS = high spin). In this work, a dinuclear cyanido-bridged Co/Fe complex, the smallest $\{Fe(\mu\text{-CN})Co\}$ moiety at the origin of the remarkable physical properties of these systems, has been designed by a rational building-block approach. Combined structural, spectroscopic, magnetic and photomagnetic studies reveal that a metal-to-metal electron transfer that can be triggered in solid state by light, temperature and solvent contents, is observed for the first time in a dinuclear complex.

The discovery in 1996 of the first photoswitchable Prussian Blue analogue,[1] $K_{0.2}Co_{1.4}[Fe(CN)_6]\cdot 6.9H_2O$, opened a new field of research in material science. The versatile molecule-based chemistry used to synthesize this Prussian Blue system motivated chemists to obtain a family of three-dimensional (3D) cyanido-bridged Co/Fe networks with different electronic behaviors tunable by external stimuli such as light and/or temperature.[2−7] The origin of the remarkable physical properties of these materials is found in the elementary $\{Fe(\mu\text{-CN})Co\}$ moiety that exhibits a reversible thermally induced and photoinduced metal-to-metal electron transfer. As a consequence, this constitutive bimetallic pair can adopt two different valence states: $\{Fe^{II}_{LS}(\mu\text{-CN})Co^{III}_{LS}\}$ and $\{Fe^{III}_{LS}(\mu\text{-CN})Co^{II}_{HS}\}$ being diamagnetic and paramagnetic respectively (LS: low spin; HS: high spin). Recently, both thermally and light induced electron transfer has been reported in two-dimensional (2D) and one-dimensional (1D) cyanido-bridged Co/Fe materials containing $\{Fe(\mu\text{-CN})Co\}$ motifs,[8−10] but so far most of the reported synthetic work in this field has been oriented toward the design of molecular complexes, able to mimic the physical properties of the 3D Prussian Blue compounds. The preparation of these discrete molecules, rather than extended networks, is of fundamental and technological interests since they may be easier to manipulate and thus to integrate into future molecule-based electronic devices. Several dinuclear[11−13] and tetranuclear[14] systems have been prepared containing diamagnetic $\{Fe^{II}_{LS}(\mu\text{-CN})Co^{III}_{LS}\}$ motifs, but it was not until 2004 that Dunbar and co-workers reported the first molecule, a pentanuclear $[Fe_2Co_3]$ complex, exhibiting a thermally induced electron transfer.[15,16] Later, in 2008 and 2010, we reported the first thermally and light switchable molecular complexes, an $[Fe_4Co_4]$ cube[17] and an $[Fe_2Co_2]$ square,[18] which can be viewed as an isolated unit cell of the cubic Prussian Blue network and an isolated face of this cubic unit, respectively. Since then, a series of related square systems have been reported, describing their different reversible thermally and light induced intramolecular electron transfer in the solid state as well as in solutions.[19−23] In our quest to obtain new molecular systems and concomitantly to reduce the size of these functional molecules, our group reported a dinuclear complex, $[\{(BBP)Fe(CN)_3\}\{Co(PY5Me_2)\}]$ ($PY5Me_2$ = 2,6-bis(1,1-bis(2-pyridyl)ethyl)pyridine; H_2BBP = 2,6-bis(benzimidazol-2-yl)pyridine) that was described as the smallest cyanido-bridged Fe/Co unit with switchable optical and magnetic properties depending on its physical state.[24] While a thermally induced Co^{II} spin crossover is observed in the solid state, an intramolecular electron transfer triggered by diprotonation of the BBP ligand at the Fe site was demonstrated in solution. Detailed electrochemistry studies showed that the ligand protonation induces a marked decrease of the redox potential difference between Fe and Co centers within the dinuclear complex, leading to the observed electron transfer. This result motivated us to design new dinuclear [FeCo] complexes exhibiting both thermally and light induced electron transfer by altering the redox potentials of the molecular precursors, as done by Bernhardt,[13] Oshio,[20] and

Received: August 7, 2014
Published: October 8, 2014

dx.doi.org/10.1021/ja508094h | J. Am. Chem. Soc. 2014, 136, 15461−15464

Mallah[25] in mixed-valence compounds. Starting with the same Co^{II} molecular module, $\{Co(PY5Me_2)\}^{2+}$, we selected the $\{(Tp)Fe^{III}(CN)_3\}^-$ building block (Tp = hydridotris(pyrazol-1-yl)borate), which can be reduced in $\{(Tp)Fe^{II}(CN)_3\}^{2-}$ around −0.81 V (vs Fc^+/Fc),[26] a redox potential that falls between those previously reported for $\{(BBP)Fe(CN)_3\}^{2-}$ and $\{(H_2BBP)Fe(CN)_3\}$ (−1.1 vs −0.46 V, respectively; Supporting Information (SI), Figure S1)[24,26] which led to paramagnetic $[Fe^{III}_{LS}(\mu\text{-CN})Co^{II}_{HS}]$ and diamagnetic $[Fe^{II}_{LS}(\mu\text{-CN})Co^{III}_{LS}]$ complexes, respectively.[24]

The room-temperature equimolar reaction of $PY5Me_2$ and $Co^{II}(CF_3SO_3)_2$ with $(Bu_4N)[(Tp)Fe^{III}(CN)_3]$ in DMF gives a dark red solution. Slow diffusion of diethyl ether vapor into this solution affords orange needles of $[\{(Tp)Fe(CN)_3\}\{Co(PY5Me_2)\}](CF_3SO_3)\cdot 2DMF$ (**1**·2DMF; 70% yield).[26]

Single-crystal X-ray diffraction studies at 180 and 90 K reveal that **1**·2DMF crystallizes in the orthorhombic *Pnma* space group (Figure 1, and SI, Table S1, Figures S3 and S4).[26] In the

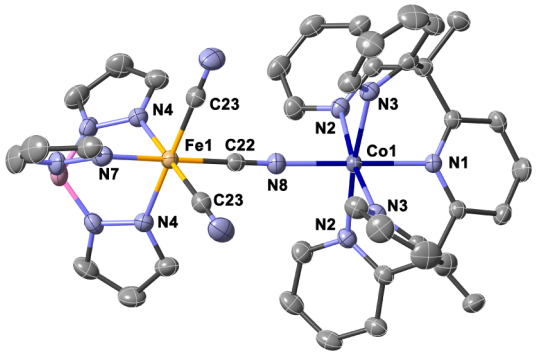

Figure 1. ORTEP-type view of the cationic complex in **1**·2DMF at 180 K. Thermal ellipsoids are depicted at the 30% probability level. All anions, lattice solvents, and hydrogen atoms are omitted for clarity. Fe, Co, N, C, and B atoms are indicated in orange, dark blue, light blue, gray, and pink, respectively.

cationic $[\{(Tp)Fe(CN)_3\}\{Co(PY5Me_2)\}]^+$ complex that resides on a mirror plane, the Fe and Co metal ions are hexacoordinated with distorted octahedral geometries (Figures 1 and SI, Figure S3),[26] and their separation (Fe···Co) is 5.063(1) Å at 180 K, which is slightly longer than 4.987(2) Å found at 90 K.

At 180 K, the two metal centers are linked by one, almost linear, cyanide ligand (Fe1−C22−N8 and C22−N8−Co1 angles are 177.6(5)° and 170.9(4)°, respectively, see SI, Table S3)[26] to form a [FeCo] pair (Figure 1). The Fe site bears two terminal cyanide ligands, and its coordination sphere is completed by three N atoms from the Tp^- ligand in facial configuration. On the other hand, the Co center completes its coordination sphere with the five N donor atoms from the $PY5Me_2$ ligand. The average Fe−C and Fe−N bonds are 1.947(5) and 1.975(4) Å, respectively, while the average Co−N_{NC} and Co−N_{py} bonds are 2.047(5) and 2.135(3) Å, respectively (SI, Table S3).[26] In addition to the bond valence analysis and the charge compensation, these structural features confirm the presence of LS Fe^{III} and HS Co^{II} metal ions in **1**·2DMF leading to a paramagnetic dinuclear complex at 180 K.

At 90 K (SI, Figure S3),[26] the cyanide bridge between Fe and Co centers is slightly more linear, with Fe1−C22−N8 and C22−N8−Co1 angles of 178.3(8)° and 171.9(8)°, respectively (SI, Table S3).[26] The average Co−N_{NC} and Co−N_{py} bond distances are notably shorter than those observed at 180 K, with values of 1.968(8) and 2.080(6) Å, respectively. However, these bond distances are too long for only diamagnetic Co^{III} ions[18−23] but are in good agreement with a mixture of both paramagnetic $[Fe^{III}_{LS}(\mu\text{-CN})Co^{II}_{HS}]$ and diamagnetic $[Fe^{II}_{LS}(\mu\text{-CN})Co^{III}_{LS}]$ dinuclear species with an approximate 1:1 ratio, as confirmed by the magnetic measurements (*vide infra*).

In the crystal structures, the +1 charge of the dinuclear complex is compensated by a $CF_3SO_3^-$ anion, while two DMF molecules are present in the crystal lattice (SI, Figure S4),[26] as confirmed by thermogravimetric analysis (TGA). The weight loss of 13 ± 1% in the 60−200 °C temperature range corresponds well to the loss of two DMF molecules (SI, Figure S8; at higher temperatures until 500 °C, **1** gradually decomposes).[26] As previously observed in related systems,[8,10,15b,20,23] the lattice solvents can strongly influence the electron-transfer properties of a complex, and therefore the properties of both **1**·2DMF and its desolvated form, **1**, have been studied.

As **1**·2DMF loses its DMF molecules extremely rapidly, the magnetic susceptibility measurements were performed on fresh crystals kept in their mother liquor (DMF/Et_2O; in red in Figure 2) between 1.8 and 250 K. At 250 K, the χT product is

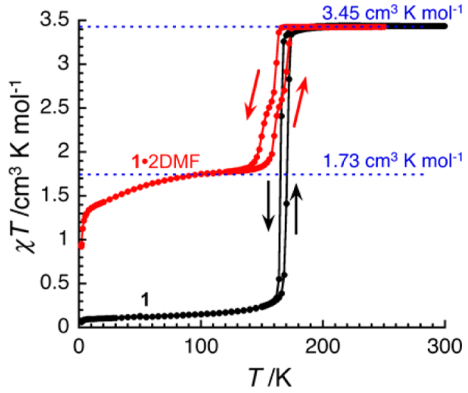

Figure 2. χT versus T plots for polycrystalline samples of **1**·2DMF (in red, from 250 to 100 K at 1 T and below 100 K at 0.1 T) and **1** (in black, from 300 to 1.8 K at 1 T) at 0.67 K/min (the lines are guides for the eye).

3.43 cm^3 K mol^{-1}, which corresponds to isolated magnetic centers, i.e., one LS Fe^{III} (S = 1/2) and one HS Co^{II} (S = 3/2) in an octahedral coordination environment. Indeed, this value is close to the value measured for the related dinuclear $[\{(BBP)Fe(CN)_3\}\{Co(PY5Me_2)\}]$ complex (3.1 cm^3 K mol^{-1}).[24] Lowering the temperature, the χT product is constant down to 165 K and then decreases sharply in two steps (at 161 and 152 K), until it reaches and stabilizes around 1.7 cm^3 K mol^{-1} at 90 K. As already suggested by single-crystal X-ray data (*vide supra*), this χT value corresponds to exactly half the χT product measured above 165 K, confirming that, in a bulk sample, only 50% of the paramagnetic $[Fe^{III}_{LS}(\mu\text{-CN})Co^{II}_{HS}]$ pairs convert into diamagnetic $[Fe^{II}_{LS}(\mu\text{-CN})Co^{III}_{LS}]$ ones. As the temperature decreases below 70 K, the χT product decreases again to reach 0.91 cm^3 K mol^{-1} at 1.8 K, as expected in the presence of the combined thermal effect of Co^{II} and Fe^{III} spin−orbit couplings[27,28] and possible antiferromagnetic coupling between LS Fe^{III} and HS Co^{II} magnetic centers through the cyanido bridge.[3] With the temperature increasing up to 130 K, the χT product increases, following the

dx.doi.org/10.1021/ja508094h | J. Am. Chem. Soc. 2014, 136, 15461−15464

same variation as seen in the cooling mode. Above 130 K, the two-step intramolecular electron transfer is observed (at 161 and 171 K) with a thermal hysteresis of about 10 K (0.67 K/min), indicating the presence of a first-order phase transition. The reversibility of the magnetic properties is confirmed above 175 K when the magnetic susceptibility recovers its initial values.

In order to obtain the desolvated analogue (**1**), **1**·2DMF was successively sonicated in diethyl ether (30 min) and kept for 24 h under vacuum at 50 °C. Complete removal of the lattice DMF solvent was confirmed by the disappearance of the intense $\bar{\nu}_{C=O}$ stretching absorption band in the solid-state IR spectrum (SI, Figure S2, at 298 K).[26] Unfortunately, based on powder X-ray diffraction, **1** is poorly crystalline, preventing its structure determination. However, the lattice DMF can be "gently", but only partially, removed by keeping **1**·2DMF in its mother liquor (DMF/Et_2O) for several days or weeks after crystallization. At a given temperature, different crystals of **1**·*n*(solv) ($n \leq 1.3$) display systematically smaller unit cells than **1**·2DMF as a consequence of DMF loss (SI, Figures S5−S7, Table S2).[26] The analysis of their crystal structures and bond distances reveals the occurrence of a partial or, in some cases (for low *n* numbers), a total thermally induced electron transfer. In this case, the presence of only the diamagnetic $[Fe^{II}_{LS}(\mu\text{-CN})Co^{III}_{LS}]$ complex at 120 K is evidenced from the Fe−C, Fe−N, Co−N_{NC}, and Co−N_{py} average bond distances of 1.892(3), 2.011(2), 1.878(3), and 1.983(2) Å, respectively. These observations indicate that **1**·2DMF can easily lose DMF molecules while maintaining the integrity of the dinuclear Fe/Co complex and favoring the occurrence of a full electron-transfer process.

In Figure 2, the magnetic properties of **1** (in black) and **1**·2DMF (in red) are compared. At 300 K, the χT product of **1** is 3.44 cm^3 K mol^{-1}, corresponding well to the paramagnetic $[Fe^{III}_{LS}(\mu\text{-CN})Co^{II}_{HS}]$ complex observed in **1**·2DMF. Upon lowering the temperature, the χT product is almost constant down to 175 K and decreases abruptly at 165 K before reaching a value of 0.21 cm^3 K mol^{-1} at 145 K, confirming the stabilization of the diamagnetic $\{Fe^{II}_{LS}(\mu\text{-CN})Co^{III}_{LS}\}$ state by a quasi-full electron transfer. In heating mode, **1** displays a sharp transition at 170 K, revealing a thermal hysteresis of about 5 K at 0.67 K/min and thus a first-order phase transition associated with the full electron transfer.

The signature of the electron transfer in **1** was also studied by solid-state optical reflectivity measurements. At 310 K, the spectrum of the paramagnetic $[Fe^{III}_{LS}(\mu\text{-CN})Co^{II}_{HS}]$ complex is composed of two bands at 490 and 850 nm (Figure 3, left, and SI, Figure S10).[26] Upon cooling, this spectrum is strongly modified in the 200−140 K temperature region, with a significant decrease in the reflectivity above 700 nm, as expected when diamagnetic $[Fe^{II}_{LS}(\mu\text{-CN})Co^{III}_{LS}]$ species are stabilized at low temperature.[15−18,21] The thermal evolution of the absolute reflectivity at 850 nm helps to visualize the optical properties (Figure 3, right, and SI, Figure S10)[26] and reveals, as observed by magnetic measurements, a thermal hysteresis (ca. 9 K at 4 K/min) associated with the thermally induced electron transfer in **1**. After 90 min of white-light irradiation of the sample at 10 K (0.4 mW/cm^2), the resulting spectrum is nearly identical to the one recorded at 310 K (SI, Figure S11),[26] demonstrating the possibility to photoinduce the electron transfer and thus the paramagnetic $[Fe^{III}_{LS}(\mu\text{-CN})Co^{II}_{HS}]$ state, at least at the surface of the sample. Upon heating, the photoinduced state relaxes around 45 K to the thermodynamic

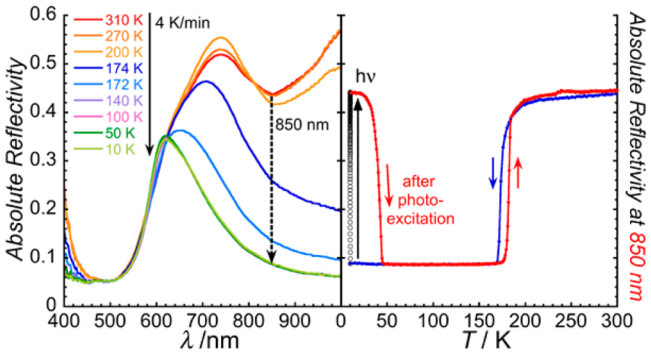

Figure 3. Left: Surface reflectivity of **1** upon cooling from 300 to 10 K (4 K/min). Right: Absolute reflectivity of **1** at 850 nm (R_{850}) with cooling (blue), heating (red), and heating after 12 h of white-light irradiation (0.4 mW/cm^2) at 10 K (red).

diamagnetic state (Figure 3, right). Additional photoexcitation experiments were performed at 10 K using a set of 14 LED sources from 1050 to 365 nm. All the 14 LEDs were able to populate the paramagnetic state (SI, Figures S12−15),[26] in agreement with the efficiency of the white light.

The electron transfer was further investigated by photomagnetic studies of **1** (Figure 4). Under white-light irradiation,

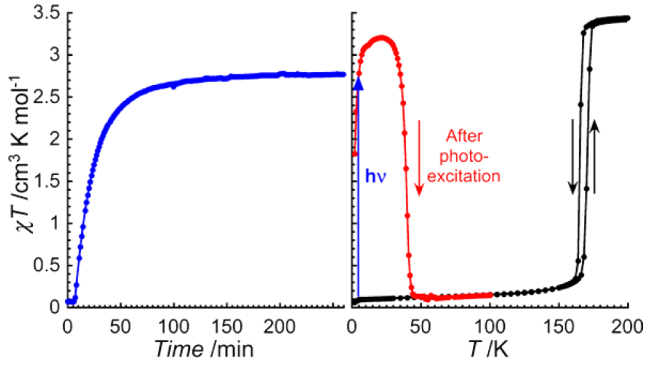

Figure 4. Left: χT versus time at 1 T under white-light irradiation (3 mW/cm^2) at 10 K. Right: χT versus temperature plots at 1 T and 0.4 K/min for **1** before (black) and after (red) white-light irradiation (3 mW/cm^2) at 10 K (the lines are guides for the eye).

the χT product at 10 K quickly increases and reaches a maximum of 2.77 cm^3 K mol^{-1} after 4 h, thus demonstrating that paramagnetic $[Fe^{III}_{LS}(\mu\text{-CN})Co^{II}_{HS}]$ complexes are photogenerated at the bulk level. From 2 to 21 K in the dark, the χT product of the photoinduced phase increased from 1.8 to 3.2 cm^3 K mol^{-1}, most likely due to the Co^{II} and Fe^{III} spin−orbit coupling[27,28] and antiferromagnetic interaction between LS Fe^{III} and HS Co^{II} magnetic sites[3] in the $[Fe^{III}_{LS}(\mu\text{-CN})Co^{II}_{HS}]$ complex (as already observed in the low-temperature phase of **1**·2DMF, Figure 2). Upon further heating, this metastable state relaxes rapidly into the thermodynamic diamagnetic phase at 45 K (Figure 4), consistent with optical reflectivity studies (Figure 3).

In summary, we have designed and synthesized the smallest [Fe(μ-CN)Co] complex that displays both thermally and light induced electron transfer in the solid state. Combined structural, spectroscopic, and magnetic studies reveal that the thermal conversion of the paramagnetic $[Fe^{III}_{LS}(\mu\text{-CN})Co^{II}_{HS}]$ complex into its diamagnetic $[Fe^{II}_{LS}(\mu\text{-CN})Co^{III}_{LS}]$ analogue is only 50% in **1**·2DMF (between 152 and 171 K), while it is

dx.doi.org/10.1021/ja508094h | J. Am. Chem. Soc. 2014, 136, 15461−15464

complete for the desolvated sample, **1** (165−170 K). Photomagnetic and optical reflectivity studies demonstrate unambiguously that the diamagnetic state of **1** can be photoconverted into the paramagnetic one by applying a simple white-light irradiation at 10 K. The thermally and light induced magnetic and optical bistability of **1** opens new possibilities to design multifunctional materials by using this moiety as a photomagnetic linker (using the remaining cyanido groups) for high-nuclearity complexes or coordination networks.

■ ASSOCIATED CONTENT

Supporting Information

Synthetic, electrochemical, spectroscopic, crystallographic, TGA, magnetic, and optical reflectivity data. This material is available free of charge via the Internet at http://pubs.acs.org.

■ AUTHOR INFORMATION

Corresponding Authors

dfli@mail.ccnu.edu.cn
mathon@icmcb-bordeaux.cnrs.fr
clerac@crpp-bordeaux.cnrs.fr

Notes

The authors declare no competing financial interest.

■ ACKNOWLEDGMENTS

The authors would like to dedicate this work to the memory of Prof. Mihail Revenco. This work was supported by the University of Bordeaux, CNRS, Aquitaine Région, IUF, ANR (ANR-12-PDOC-0038), NNSF of China (21172084 and 20802022), the Program for New Century Excellent Talents in University of China (NCET-10-040), and CCNU (CCNU13F006, CCNU14Z01001, CCNU11C01002). The authors thank E. Hillard, P. Rosa, D. Denux, A. Derré, and S. M. Holmes for fruitful discussions.

■ REFERENCES

(1) Sato, O.; Iyoda, T.; Fujishima, A.; Hashimoto, K. *Science* **1996**, *272*, 704.
(2) Bleuzen, A.; Lomenech, C.; Escax, V.; Villain, F.; Varret, F.; Cartier dit Moulin, C.; Verdaguer, M. *J. Am. Chem. Soc.* **2000**, *122*, 6648.
(3) (a) Champion, G.; Escax, V.; Cartier dit Moulin, C.; Bleuzen, A.; Verdaguer, M. *J. Am. Chem. Soc.* **2001**, *123*, 12544. (b) Goujon, A.; Roubeau, O.; Varret, F.; Dolbecq, A.; Bleuzen, A.; Verdaguer, M. *Eur. Phys. J. B* **2000**, *14*, 115.
(4) Cartier dit Moulin, C.; Villain, F.; Bleuzen, A.; Arrio, M.-A.; Sainctavit, P.; Lomenech, C.; Escax, V.; Baudelet, F.; Dartyge, E.; Gallet, J.-J.; Verdaguer, M. *J. Am. Chem. Soc.* **2000**, *122*, 6653.
(5) Escax, V.; Bleuzen, A.; Cartier dit Moulin, C.; Villain, F.; Goujon, A.; Varret, F.; Verdaguer, M. *J. Am. Chem. Soc.* **2001**, *123*, 12536.
(6) Sato, O.; Einaga, Y.; Fujishima, A.; Hashimoto, K. *Inorg. Chem.* **1999**, *38*, 4405.
(7) Shimamoto, N.; Ohkoshi, S.-i.; Sato, O.; Hashimoto, K. *Inorg. Chem.* **2002**, *41*, 678.
(8) Liu, T.; Zhang, Y.-J.; Kanegawa, S.; Sato, O. *Angew. Chem., Int. Ed.* **2010**, *49*, 8645.
(9) Liu, T.; Zhang, Y.-J.; Kanegawa, S.; Sato, O. *J. Am. Chem. Soc.* **2010**, *132*, 8250.
(10) Hoshino, N.; Iijima, F.; Newton, G. N.; Yoshida, N.; Shiga, T.; Nojiri, H.; Nakao, A.; Kumai, R.; Oshio, H. *Nat. Chem.* **2012**, *4*, 921.
(11) Bernhardt, P. V.; Martinez, M. *Inorg. Chem.* **1999**, *38*, 424.
(12) Bernhardt, P. V.; Macpherson, B. P.; Martinez, M. *Inorg. Chem.* **2000**, *39*, 5203.
(13) Bernhardt, P. V.; Macpherson, B. P.; Martinez, M. *J. Chem. Soc., Dalton Trans.* **2002**, 1435.
(14) Oshio, H.; Onodera, H.; Tamada, O.; Mizutani, H.; Hikichi, T.; Ito, T. *Chem.—Eur. J.* **2000**, *6*, 2523.
(15) (a) Berlinguette, C.; Dragulescu-Andrasi, A.; Sieber, A.; Galàn-Mascaròs, J. R.; Güdel, H.-U.; Achim, C.; Dunbar, K. R. *J. Am. Chem. Soc.* **2004**, *126*, 6222. (b) Berlinguette, C.; Dragulescu-Andrasi, A.; Sieber, A.; Güdel, H.-U.; Achim, C.; Dunbar, K. R. *J. Am. Chem. Soc.* **2005**, *127*, 6766.
(16) Later, in 2011, this complex was reported to display a photoinduced intramolecular electron transfer: Funck, K. E.; Prosvirin, A. V.; Mathonière, C.; Clérac, R.; Dunbar, K. R. *Inorg. Chem.* **2011**, *50*, 2782.
(17) Li, D.; Clérac, R.; Roubeau, O.; Harté, E.; Mathonière, C.; Le Bris, R.; Holmes, S. M. *J. Am. Chem. Soc.* **2008**, *130*, 252.
(18) Zhang, Y.; Li, D.; Clérac, R.; Kalisz, M.; Mathonière, C.; Holmes, S. M. *Angew. Chem., Int. Ed.* **2010**, *49*, 3752.
(19) Mercurol, J.; Li, Y.; Pardo, E.; Risset, O.; Seuleiman, M.; Rousselière, H.; Lescouëzec, R.; Julve, M. *Chem. Commun.* **2010**, *46*, 8995.
(20) Nihei, M.; Sekine, Y.; Suganami, N.; Nakazawa, K.; Nakao, A.; Nakao, H.; Murakami, Y.; Oshio, H. *J. Am. Chem. Soc.* **2011**, *133*, 3592.
(21) (a) Siretanu, D.; Li, D.; Buisson, L.; Bassani, D. M.; Holmes, S. M.; Mathonière, C.; Clérac, R. *Chem.—Eur. J.* **2011**, *17*, 11704. (b) Zhang, Y.-Z.; Ferko, P.; Siretanu, D.; Ababei, R.; Rath, N. P.; Shaw, M. J.; Clérac, R.; Mathonière, C.; Holmes, S. M. *J. Am. Chem. Soc.* **2014**, DOI: 10.1021/ja508280n.
(22) Mondal, A.; Li, Y.; Seuleiman, M.; Julve, M.; Toupet, L.; Buron-Le Cointe, M.; Lescouëzec, R. *J. Am. Chem. Soc.* **2013**, *135*, 1653.
(23) Cao, L.; Tao, J.; Gao, Q.; Liu, T.; Xia, Z.; Li, D. *Chem. Commun.* **2014**, *50*, 1665.
(24) Jeon, I.-R.; Calancea, S.; Panja, A.; Piñero Cruz, D. M.; Koumousi, E. S.; Dechambenoit, P.; Coulon, C.; Wattiaux, A.; Rosa, P.; Mathonière, C.; Clérac, R. *Chem. Sci.* **2013**, *4*, 2463.
(25) Rogez, G.; Marvillers, A.; Sarr, P.; Parsons, S.; Teat, S. J.; Ricard, L.; Mallah, T. *Chem. Commun.* **2002**, *14*, 1460.
(26) See Supporting Information.
(27) Zadrozny, J. M.; Freedman, D. E.; Jenkins, D. M.; Harris, T. H.; Iavarone, A. T.; Mathonière, C.; Clérac, R.; Long, J. R. *Inorg. Chem.* **2010**, *49*, 8886.
(28) (a) Lescouëzec, R.; Vaissermann, J.; Lloret, F.; Julve, M.; Verdaguer, M. *Inorg. Chem.* **2005**, *41*, 5943. (b) Li, D.; Parkin, S.; Wang, G.; Yee, G. T.; Holmes, S. M. *Inorg. Chem.* **2006**, *45*, 1951.